EVALUATION OF MARS ENTRY RECONSTRUCTED TRAJECTORIES BASED ON HYPOTHETICAL 'QUICK-LOOK' ENTRY NAVIGATION DATA

P. R. (Rick) Pastor[1], Robert H. Bishop[2]
University of Texas Center for Space Research, Austin, Texas, 78712

Scott A. Striepe[3]
NASA Langley Research Center
Hampton, Virginia, 23681

Abstract

A first order simulation analysis of the navigation accuracy expected from various 'Navigation Quick-Look' data sets is performed. Here 'quick-look' navigation data are observations obtained by hypothetical telemetried data transmitted 'on the fly' during a Mars probe's atmospheric entry. In this simulation study, navigation data consists of 3-axis accelerometer sensor and attitude information data. Three entry vehicle guidance types are studied: I. a Maneuvering entry vehicle (as with Mars '01 guidance where angle of attack and bank angle are controlled); II. Zero angle-of-attack controlled entry vehicle (as with Mars '98); and III. Ballistic, or spin stabilized entry vehicle (as with Mars Pathfinder);. For each type, sensitivity to progressively under sampled navigation data and inclusion of sensor errors are characterized. Attempts to mitigate the reconstructed trajectory errors, including smoothing, interpolation and changing integrator characteristics are also studied.

INTRODUCTION

This paper is a first order simulation analysis of the navigation accuracies expected from processing 'Navigation Quick-Look' data, to generate reconstructed Mars entry

[1] Research Engineer/Scientist
[2] Associated Professor, Department of Aerospace Engineering and Engineering Mechanics
[3] Aerospace Engineer, Vehicle Analysis Branch, Aerospace Systems, Concepts and Analysis Competency Division

trajectories. Navigation 'quick-look' data is hypothetically telemetried navigation data transmitted 'on the fly' during a probe's Mars entry. It must be stressed that the physical plausibility of this transmission is not the object of this paper, but rather what would be this data set's utility *if* it were available. In this simulation study, navigation data consists of 3-axis accelerometer data and attitude information. The simulation data, including corruptions, is used to generate entry trajectory reconstruction's which are each compared with the simulated trajectories (considered to be true states). Three entry vehicle configurations are studied (as shown in Table 1): I. a Maneuvering entry vehicle (as with Mars '01 guidance where angle of attack and bank angle are controlled); II. Zero angle-of-attack controlled entry vehicle (as with Mars '98); and III. Ballistic, or spin stabilized entry vehicle (as with Mars Pathfinder). In each "guidance" case above, the sensitivity to various corruptions are parametrically characterized. The corruptions considered are: varying the telemetry data frequencies (i.e., progressive under sampling); and, inclusion of expected accelerometer and attitude measurement errors.

Table 1. Study Types: Mars Entry Guidance and Control Configrations

Type	Example Mission	Brief Description
I. Guided Lifting Trajectory	Mars '01 Lander	Active guidance with RCS control to adjust angle of attack and bank angle
II. Unguided but Controlled	Mars Polar Lander	RCS thrusters use to zero out angle-of-attack (AOA)
III. Ballistic Spinner	Mars PathFinder	Zero nominal lift, spin stabilized

As discussed by many investigators, current planetary exploration missions are characterized by campaigns of low-cost, interdependent spacecraft with typical development time of years rather than decades. One means of achieving the reduction in mission cost is through the use of "aeroassist" techniques that make use of atmospheric forces to reduce typical propellant usage over traditional propulsive capture, orbit, and landing scenarios. Two subsets of aeroassist applications include direct entry and precision landing. Mars Pathfinder's direct Entry, Decent and Landing (EDL) on July 4, 1997 is an example of the successful use of the direct entry method. Current and future robotic missions will likely make use of the direct entry decent and landing techniques. In addition, lander missions will operate EDL scenarios with progressively more elaborate operational guidance and control techniques to satisfy increasingly stringent precision landing requirements.

As part of the direct entry missions, a *post-landing* accurate reconstruction of the entry trajectories, often referred to as a Best Estimated Trajectory - or BET, is calculated. This product is used to study the performance of the spacecraft's EDL sequence, principally the crucial parachute deploy, as well as the state of the Mars atmospheric profile along its entry path. For the Mars Pathfinder mission, and as part of the Atmospheric Science Investigation /Meteorology (ASI/MET) experiment, Braun et al.[2], computed a BET using all available flight data. The dominant observations were from the onboard 3-axis

accelerometers that provided a direct measure of the non-conservative accelerations, principally drag. These accelerations were combined with other sensor measurements and modeled conservative gravity forces to estimate the entry trajectory. Use of the lateral accelerometer data was limited by the lack of gyro attitude data. The investigation in ref. 2 was able to assess the Pathfinder system performance through the hypersonic entry and the parachute deployment using observed spin rates and an inferred total angle-of-attack profile, as well as estimate atmospheric density and temperature profiles.

For this present work the focus is on employing a very rarefied set of the on-board measured navigation data transmitted 'on the fly' during the actual Mars entry trajectory. This "quick-look" navigation data being used to determine, in near real-time, a coarse accuracy reconstructed trajectory and possibly entry navigation health. In comparison, high accuracy BETs would involve a multi-level solution methodology performed with all available flight observations. This "full-rate" data includes high rate accelerometer data from an Inertial Measurement Unit (IMU) accelerometer, radar altitude and velocity information during the parachute and terminal decent phases, on-board guidance, commanded controls and landed position as well as entry navigation conditions. Solution methods for BETs include dead-reckoning, batch, Kalman filtering and smoothing techniques, which are in part used to test the iterative, hierarchical and cross-checking solution scenarios. For accelerometer data in the BET solution, scale-factor, bias, non-orthogonality and noise effects are included as corrections, errors, or optionally estimated. Similarly, included in a BET solution process are the cruise navigation entry state conditions and their associated full covariance description.

So, in comparison "Quick Look" reconstructed trajectories process a limited data set with relatively simple processing; thus their solutions are not meant as a replacement for the more thorough and likely higher accuracy BET solutions.

PROCESSING CONFIGURATION

Simulation Configuration

The simulation used to generate entry trajectory data for these analyses is the six degree-of-freedom Atmospheric Entry Simulation. This software was used to evaluate guidance algorithms proposed for the Mars Surveyor Program 2001 Lander. Reference 1 explains this simulation and how it was used for Monte Carlo-type dispersion runs with the MSP'01 Lander mission. This high fidelity, 6DOF simulation includes models that emulate the entry flight systems. The dispersed quantities include aerodynamic, atmosphere, control system, IMU, initial state, and mass property data. Values used from the MSP'01 Lander mission are shown in Table 2.

For these analyses, a nominal and several perturbed cases were evaluated for the MSP'01 type (guided using bank angle modulation) entry trajectory. The values generated included quantities which were adjusted to simulate noise and other characteristics of IMU data returned after entry. The states generated by the simulation were used as the true trajectory, while the quantities provided by the IMU model were treated as the observations.

Figure 1 shows the sensed accelerations (provided by the accelerometer data from the IMU model) in the vehicle body axes for a nominal MSP'01 type guided entry. The angle of attack and bank angle time histories for this entry are illustrated in figure 2. The atmospheric data used for this entry simulation is shown in figure 3. Of these three sets of data, only the sensed accelerations are included in the data used to reconstruct the trajectory. The other figures indicate the conditions encountered and nominal attitude during the trajectory.

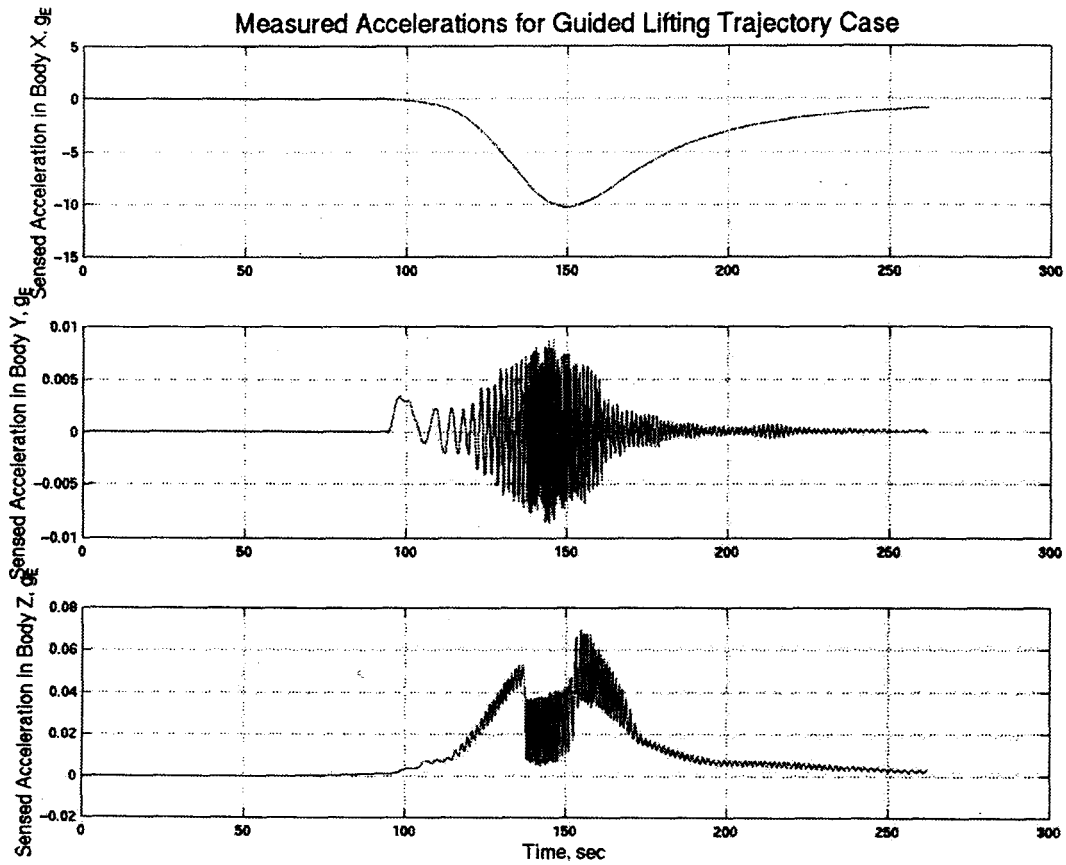

Figure 1. Measured Accelerations for MSP'01 type guided entry.

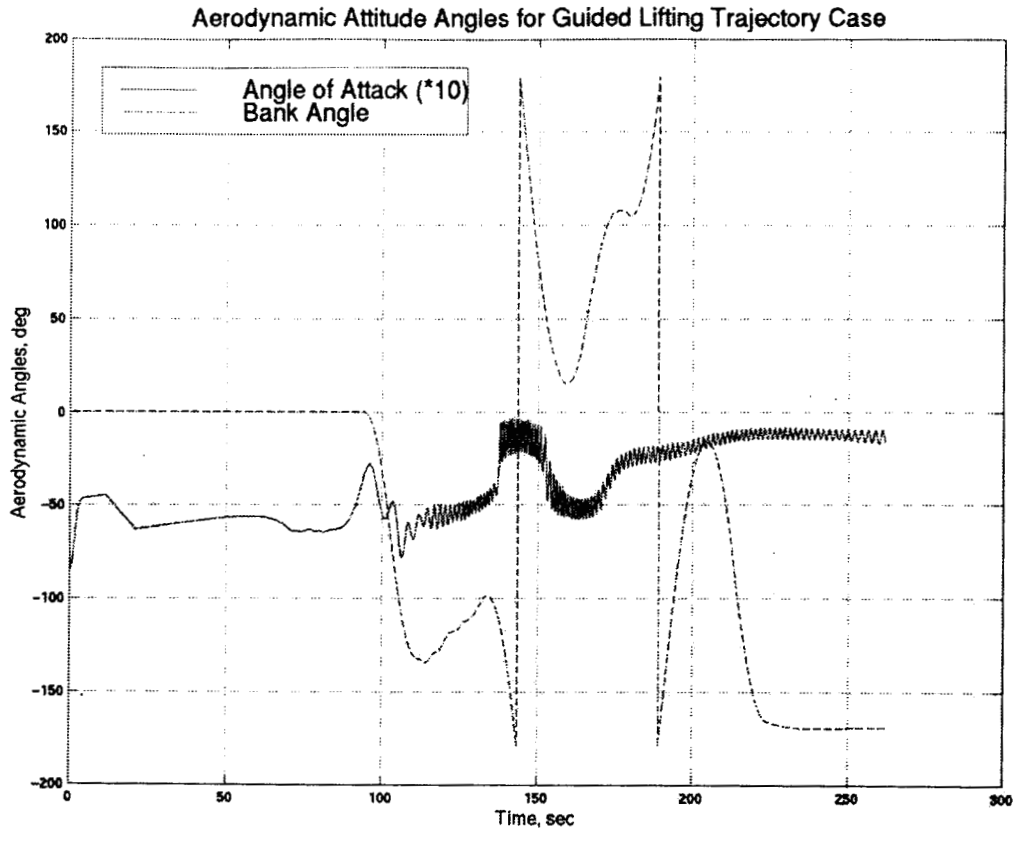

Figure 2. Aerodynamic Angles for Guided Entry Trajectory.

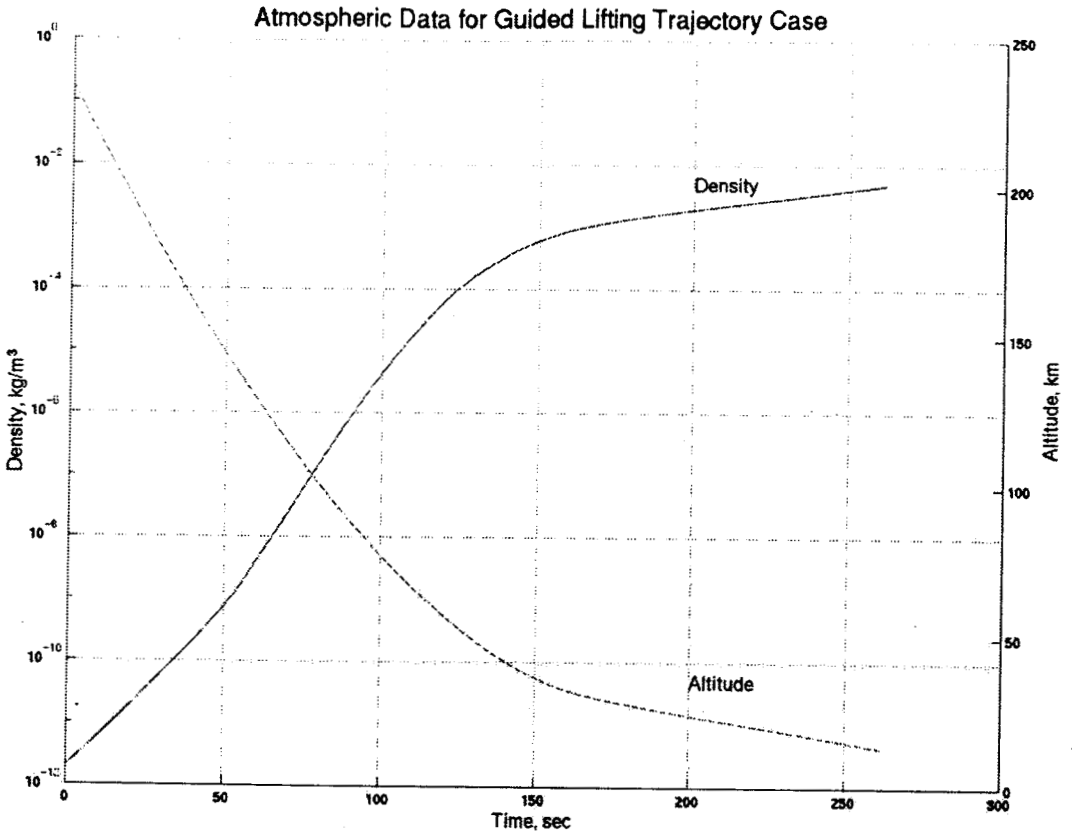

Figure 3. Atmospheric Data for Guided Entry Trajectory.

Table 2. MSP'01 Lander Mission Dispersions[1]

Quantity	Nominal Value	Distribution Type	3-σ or min/max
Mission Uncertainty			
Initial Bank, deg	0.0	Gaussian	5.0
Initial Angle of Attack, deg	-14.7	Gaussian	5.0
Initial Sideslip Angle, deg	0.0	Gaussian	5.0
Initial Pitch rate, deg/sec	0.0	Gaussian	5.0
Initial Roll rate, deg/sec	0.0	Gaussian	5.0
Initial Yaw rate, deg/sec	0.0	Gaussian	5.0
Aerodynamic Uncertainty			
Axial Force Coeff Incr (free molecular)	0	Gaussian	10 %
Normal Force Coeff Incr (FM)	0	Gaussian	10 %
Axial Force Coeff Incr (Mach > 10)	0	Gaussian	3 %
Normal Force Coeff Incr (Mach > 10)	0	Gaussian	5 %
Axial Force Coeff Incr (Mach < 5)	0	Gaussian	10 %
Normal Force Coeff Incr (Mach < 5)	0	Gaussian	8 %
Pitch Moment Coeff Incr (FM)	0	Gaussian	10 %
Pitch Moment Coeff Incr (Mach > 10)	0	Gaussian	8 %
Pitch Moment Coeff Incr (Mach< 5)	0	Gaussian	10 %
Pitch Damping Coeff Incr (Mach > 10)	0	Gaussian	15 %
Pitch Damping Coeff Incr (Mach< 5)	0	Gaussian	15 %
Mass Property Uncertainty			
Mass, kg	523.0	Gaussian	2.0
Axial CG position, m	0.7155	Gaussian	0.010
Lateral CG position, m	0.0170	Gaussian	0.005
Lateral CG offset direction, deg	0	Uniform	0/180
Ixx, kg-m^2	261.0	Gaussian	5 %
Iyy, kg-m^2	194.4	Gaussian	5 %
Izz, kg-m^2	212.3	Gaussian	5 %
Ixy, kg-m^2	0.0	Gaussian	1.0
Ixz, kg-m^2	0.0	Gaussian	3.0
Iyz, kg-m^2	0.0	Gaussian	15.0
Atmospheric Uncertainty			
Initial Seed Value	0	Uniform	1/29999
Update distance, km	0.5	Uniform	0.5/5.0
Opacity Factor (TAU)	1.0	Uniform	0.3/1.6
Control System Uncertainty			
Roll/yaw thrusters, lb	1.0	Gaussian	5 %
Pitch thrusters, lb	5.2	Gaussian	5 %
IMU Uncertaintiy			
Initial Seed Value	0	Uniform	1/29999
Initial angular misalignment, arcsec	0	Gaussian	126
gyro bias drift, deg/hr	0	Gaussian	0.03
gyro scale factor, ppm	0	Gaussian	99
gyro nonorthogonality, ppm	0	Gaussian	60
gyro random walk (PSD), deg/rt-hr	0	Gaussian	0.03
accelerometer bias, milligees	0	Gaussian	0.18
accelerometer scale factor, ppm	0	Gaussian	300

Dead Reckoning Reconstruction and Comparison Configuration

Synthetic observations from the AES simulator, discussed above, are passed after preprocessing into a "Dead Reckoning" propagator to generate the reconstructed entry trajectory. The process is diagramed in figure 4. The preprocessing of the AES 0.1s "raw" data includes appropriate down-sampling to measure the effect of "Quick-Look" (QL) NAV data provides at varying data rates. After the DR propagator receives the input NAV data, it employs a multistep, second degree Krogh-Shampine-Gordon (KSG)[3] (nominally of seventh order) numerical integrator to generate a "QL Reconstruction" trajectory. Note that the integrator runs with a step size consistent with NAV accelerometer data downstream from the down-sample preprocessor; in comparison, the upstream AES NAV generator employs a fourth order Runge-Kutta integrator running with a 0.01s step size. Preprocessing of the raw AES data also includes smoothing and interpolation. Lastly, to compute the accuracy of the reconstruction trajectories, the DR states are differenced with the corresponding AES "Truth" trajectory to plot relative differences in various projections.

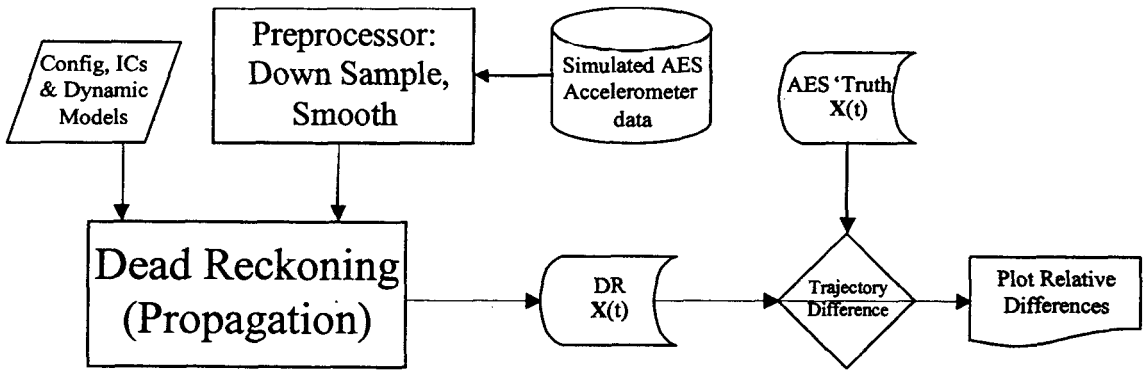

Figure 4. Diagram of "Dead Reckoning" Processing Configuration.

RESULTS

Type 1: Guided Entry

Three dimensional differences between DR reconstructed solutions and the AES truth trajectories are shown in figure 6 for successively rarified QL NAV data rates. Though comparisons are shown for QL NAV data including noise, very little difference is observed when non-noise (perfect) data is processed.

Effects observed in positions

Position differences remain small, less than 20 meters in the root sum square (RSS) of the differences. At approximately 130-140 seconds into flight the position difference increase linearly with generally increasing slopes (i.e., a faster rate in the amount of difference) as the NAV observation data frequency decreases. The onset of difference

growth at 130-140 seconds corresponds to the time of maximum vehicle deceleration which peaks at near -100 meters/sec^2 150 seconds into entry. (Times are measured relative to "atmospheric entry minus 60 sec".)

Differences in the relative up, and along-track (or, alternately in the radial, and transverse) positions expand to approximately +/- 500 meters; again with size of the differences being proportional to the sparsity (frequency decreasing) of the employed NAV observation data. Differences in the cross-track are slightly larger, expanding to approximately +/- 800 meters. Except for the larger size of the cross-track differences, relative to either the up, or along-track (or, alternately in the radial or transverse), no strong indication is observed in any single difference "channel" which would uniquely show a correlation signature between the size of the difference and the frequency of the NAV observations. That is, no single projection difference "channel" uniquely, best, or first indicates a difference proportional to the frequency of the observations. Rather, all projections show differences with slopes increasing as the data becomes more sparse. All differences begin during maximum change in acceleration which occurs over the interval of 130-140 seconds. Generally speaking, the differences for each observation frequency solution "path" increases monotonically and linearly with time.

Effects observed in velocities

As with position, velocity differences remain small, generally less than 0.1 m/sec, until approximately 130-140 seconds into the flight. At that time they generally inflate (chaotically) until approximately 170 seconds when they dampen down to steady-state biases for a given frequency solution "path". Again, as with position, the size of the differences increase with the decreasing frequency of the measurements employed by a solution.

Velocity differences, are largest in the cross-track projection at approximately +/- 8 m/sec; in the up, or along-track (or, alternately the radial or transverse) differences are approximately +/- 6 m/sec. Again, as with position, no most dominate velocity difference "channel" is observed.

In general, entry solutions with measurements frequencies of 0.4 seconds or less have bounded differences, over the entire span of the flight. In position, this difference is less than 30 meters. For velocity, it is below 1.5 m/sec.

Effect of Accelerometer Measurement Noise

Runs made with noise data, synthesized by the generating AES simulator, produce a reconstruction trajectory which produce differences (compared to the "true" states) that are generally similar or even *smaller* than for the non-noised (perfect) data. Most of this difference is to due smaller deviations in the along-track, or along the velocity vector, direction, and to a lesser extent in the "upward" direction. We believe that these smaller differences are because the effect of the simulated sensor noise is at high enough frequencies, relative to the downsampled accelerometer data, that it effectively smoothes the data and thus produces smaller differences. Without the smoothing, the data contains frequencies higher that can be accommodated by the DR's 7th order integrator.

Apparently noisy data, apparently, does not significantly impact the dead-reckoning approach using down-sampled "quick-look" NAV Data.

Effect of Smoothing High Frequency Signal in QL NAV Data

In an attempt to empirically explain the slope in the positions and bias in the velocities, several additional parametric variation runs were performed. These runs included varying the DR integrator order, operating on simulated QL NAV data without included noise, smoothing through the QL NAV data, and reinterpolating to the raw data's high rate frequency.

The observed structure in the AES guidance '01 type measured accelerations is shown in figure 7. Very little effect from any of these parametric variations were observed. Apparently, as the QL NAV data becomes increasingly rarified (data frequency is decreased), this down-sampling of the accelerometer observations results in loss of information content and the resulting DR propagation proceed along an increasingly divergent integration 'path'. Since the principal acceleration is from the non-conservative aerodynamic drag, the diverging DR reconstructed trajectory can never 'catch-up' with the "true" trajectory.

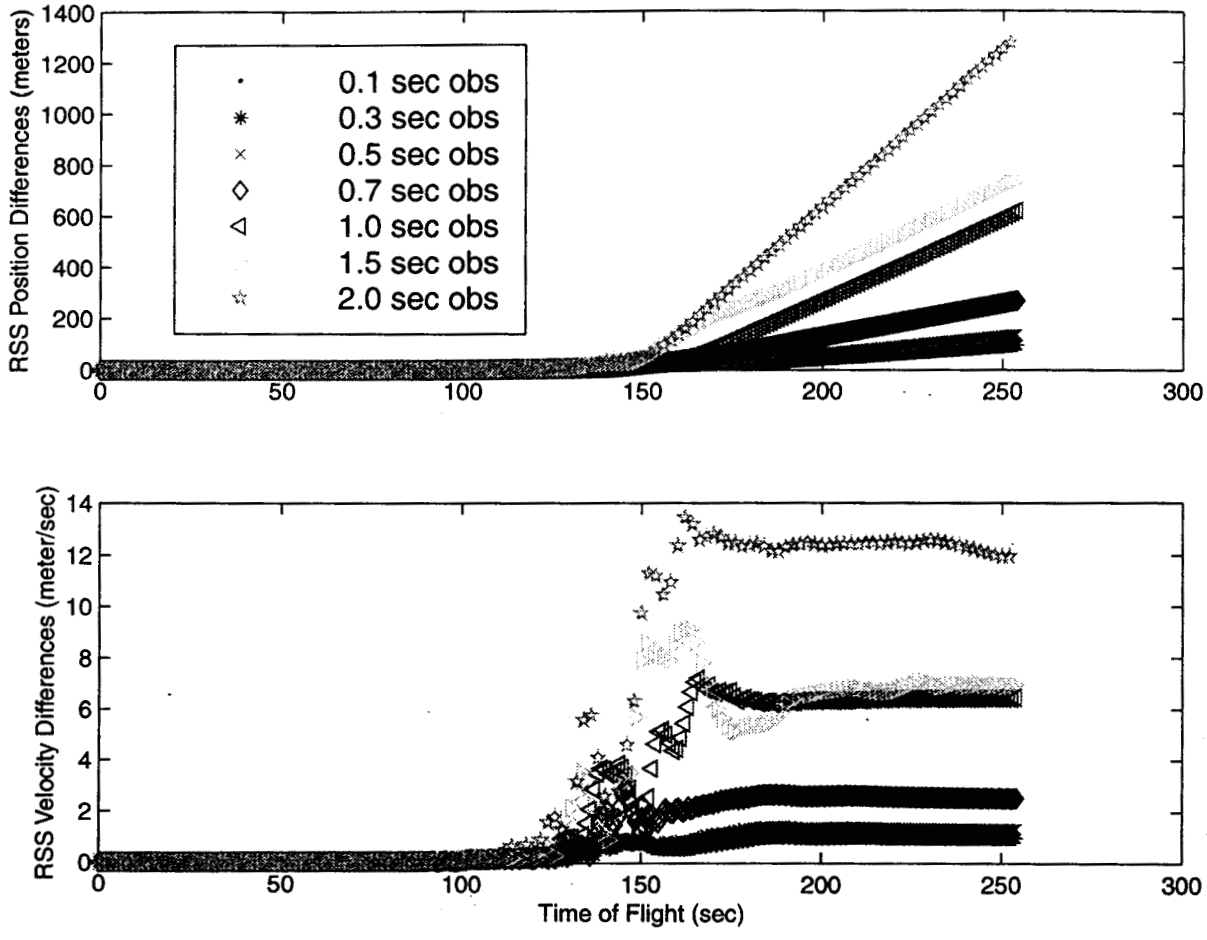

Figure 6. Reconstruction Sensitivity to Varying "Quick-Look" NAV Data Rate: "Guided" Type ('01 Mission)

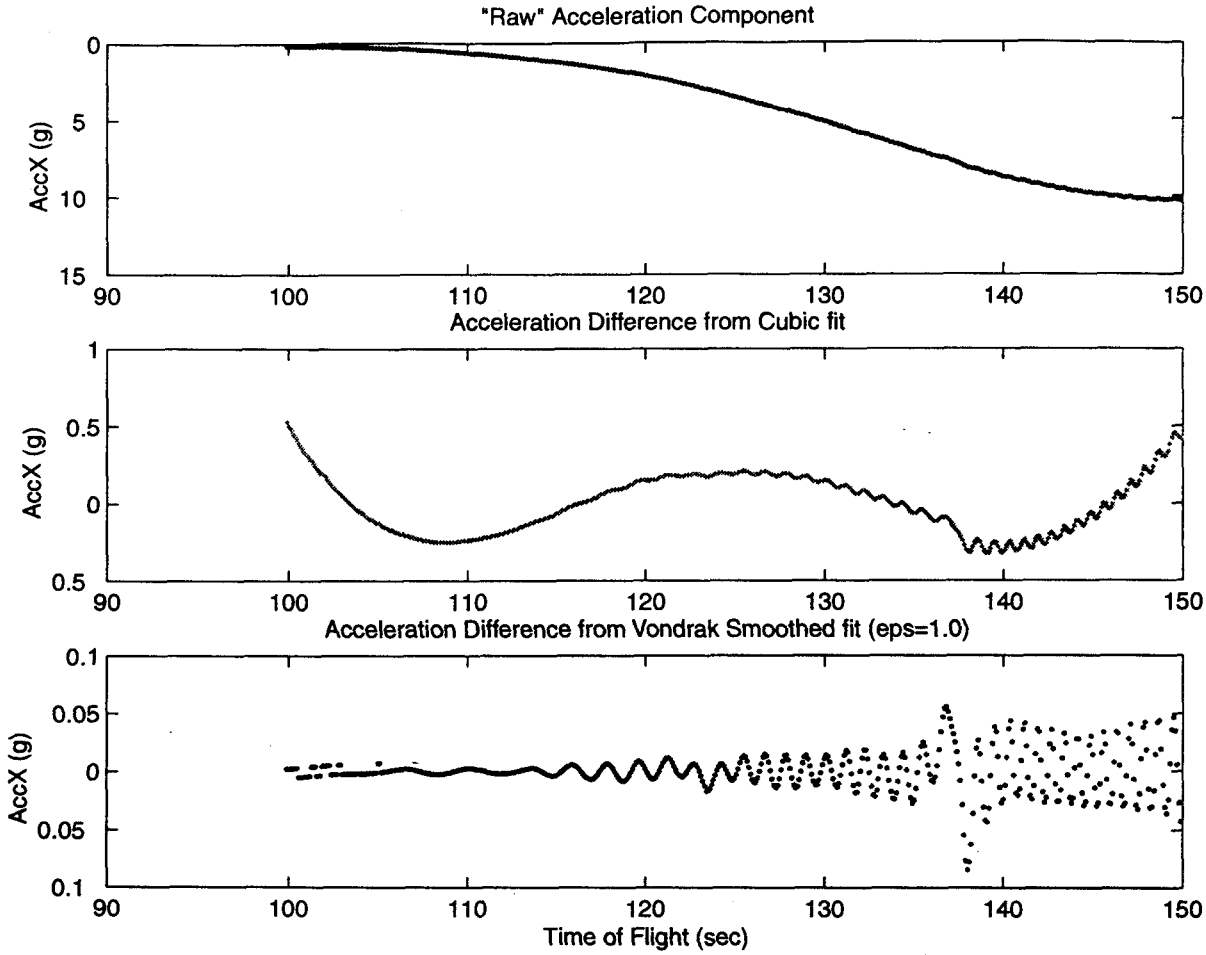

Figure 7. Plot of Synthetic AES Acceleration Data's High Frequency Structure and Applied Smoothing in Reconstruction: : "Guided" Type ('01 Mission)

Case 2: AOA Controlled ;MPL Type

As shown in figure 8, there exists much less high frequency signal in the "raw" MPL type acceleration time series, as compared with the guided '01 accelerations plotted in figure 7. This reduction is due to much smaller variations in angle-of-attack angles, and consequently less lift forces experienced by the MPL type guidance. Thus as expected smaller reconstruction differences, as shown in figure 9 are observed (as in comparison with figure 6).

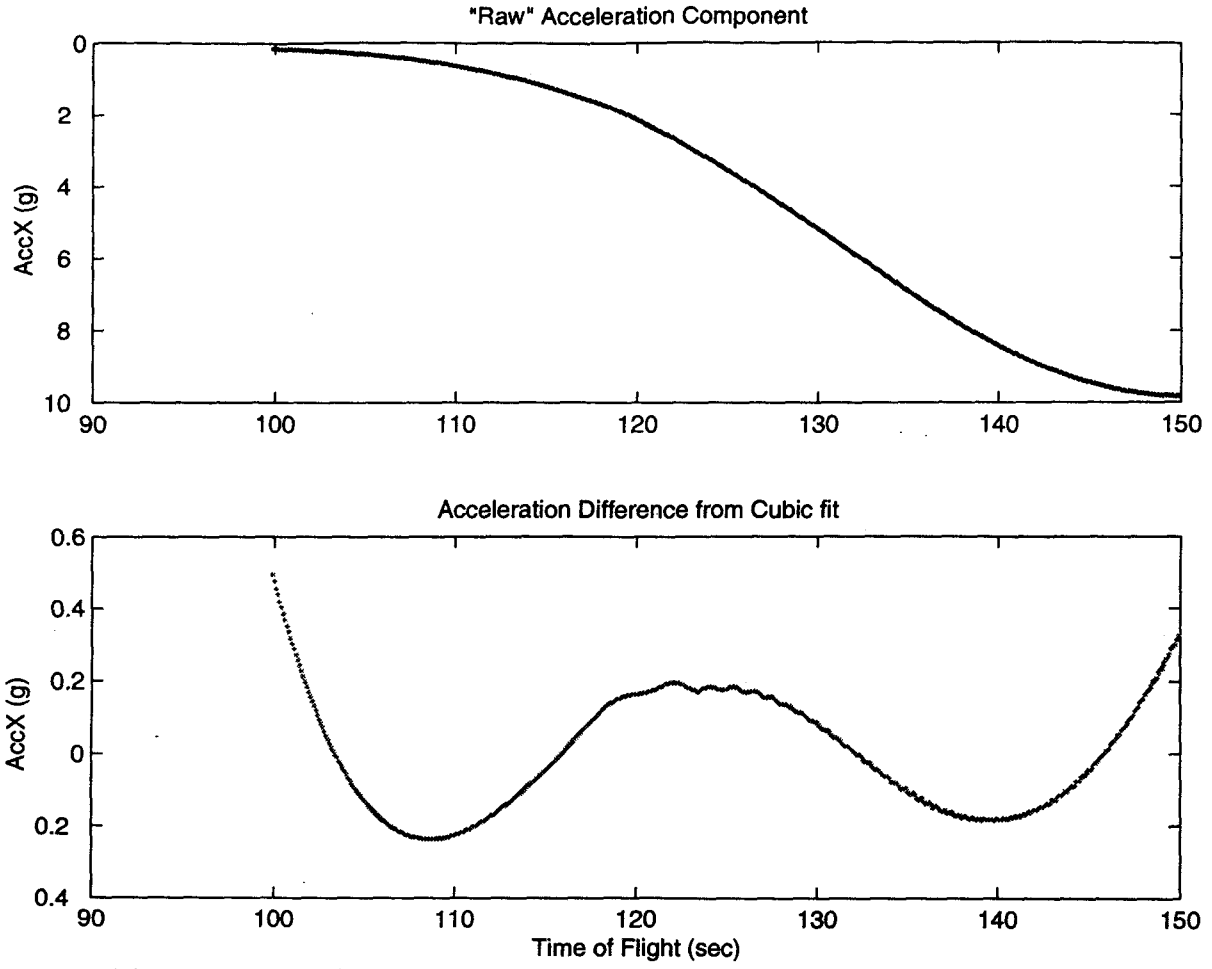

Figure 8. Plot of AES Simulated Acceleration High Frequency: MPL Type

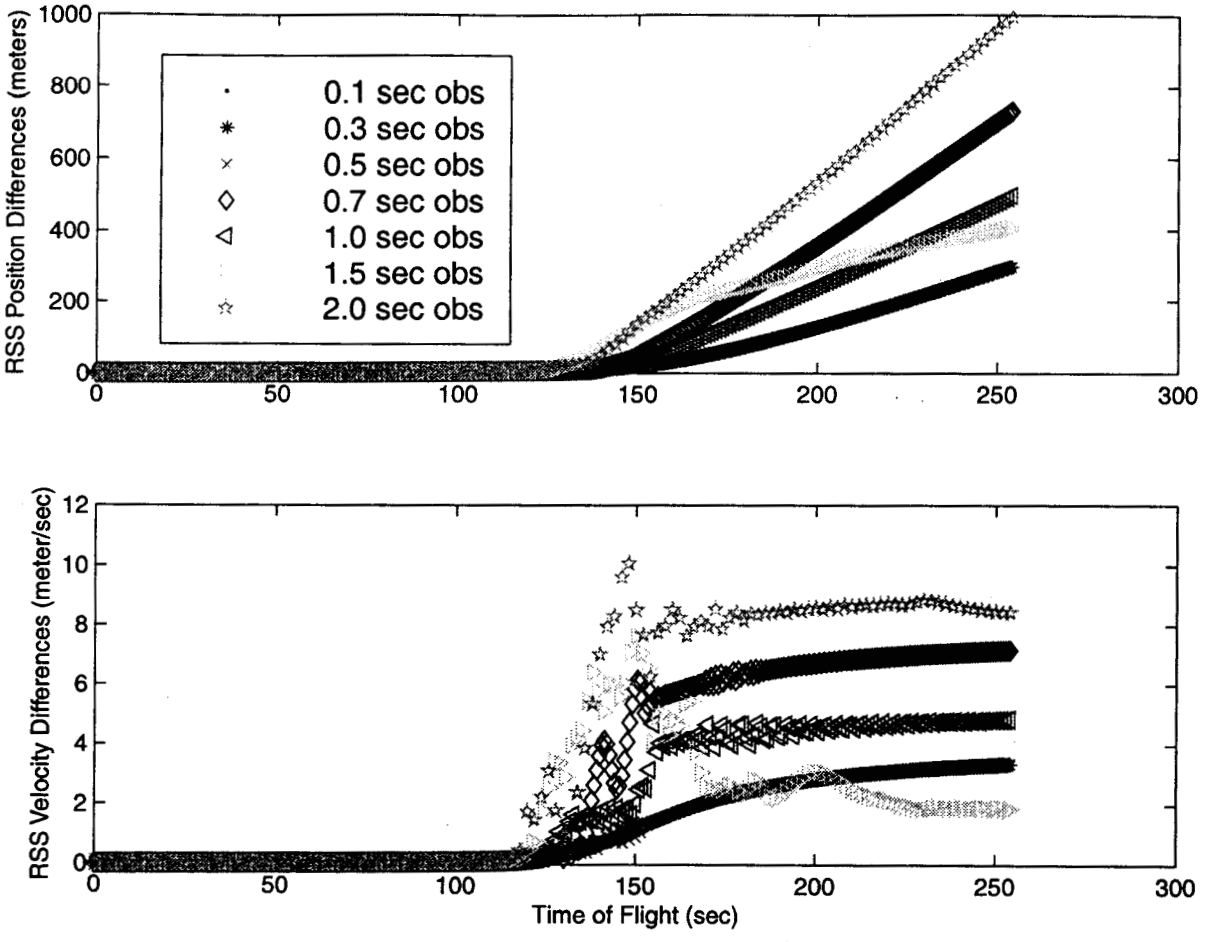

Figure 9. Reconstruction Sensitivity to Varying "Quick-Look" NAV Rate (Noisy) Data: MPL Type

Case 3: Ballistic, Spin Stabilized Entry

The ballistic, spin stabilized, MPF type incorporates the smallest magnitude lift forces of any of the three 'guidance' types analyzed. As expected, as shown from figure 10, maximum RSS position differences decrease from approximately 1.0 (in figure 9) to 0.7 Km for the MPF type; velocity differences show a similar, but not as dramatic, improvement. From the striking improvement in both position and velocity observed for the 1.5s observation case, there appears to be a correlation between the "Quick-Look" measurement rate and the natural oscillation frequency of the 70deg aerobody.

In order to compare the range of differences observed between reconstructed and truth-trajectories for the various guidance types, the difference in Truth Trajectories for the '01 Guided and MPL types – relative to the least guided MPF type is plotted in figure 11. When compared, it is observed that the total truth-trajectory differences between the guidance types is almost always larger than the reconstruction errors from figures 6, 9, and 10.

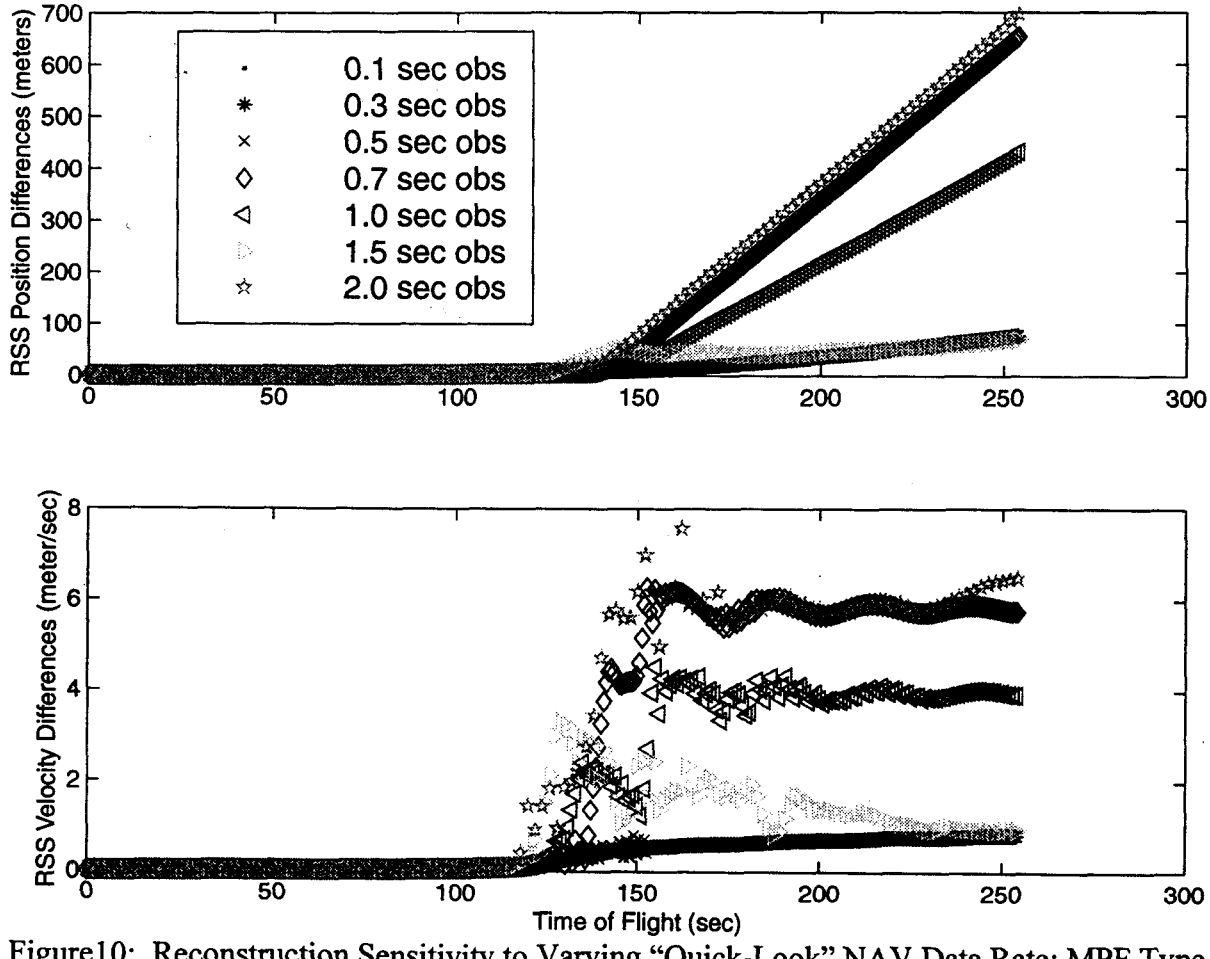

Figure10: Reconstruction Sensitivity to Varying "Quick-Look" NAV Data Rate: MPF Type

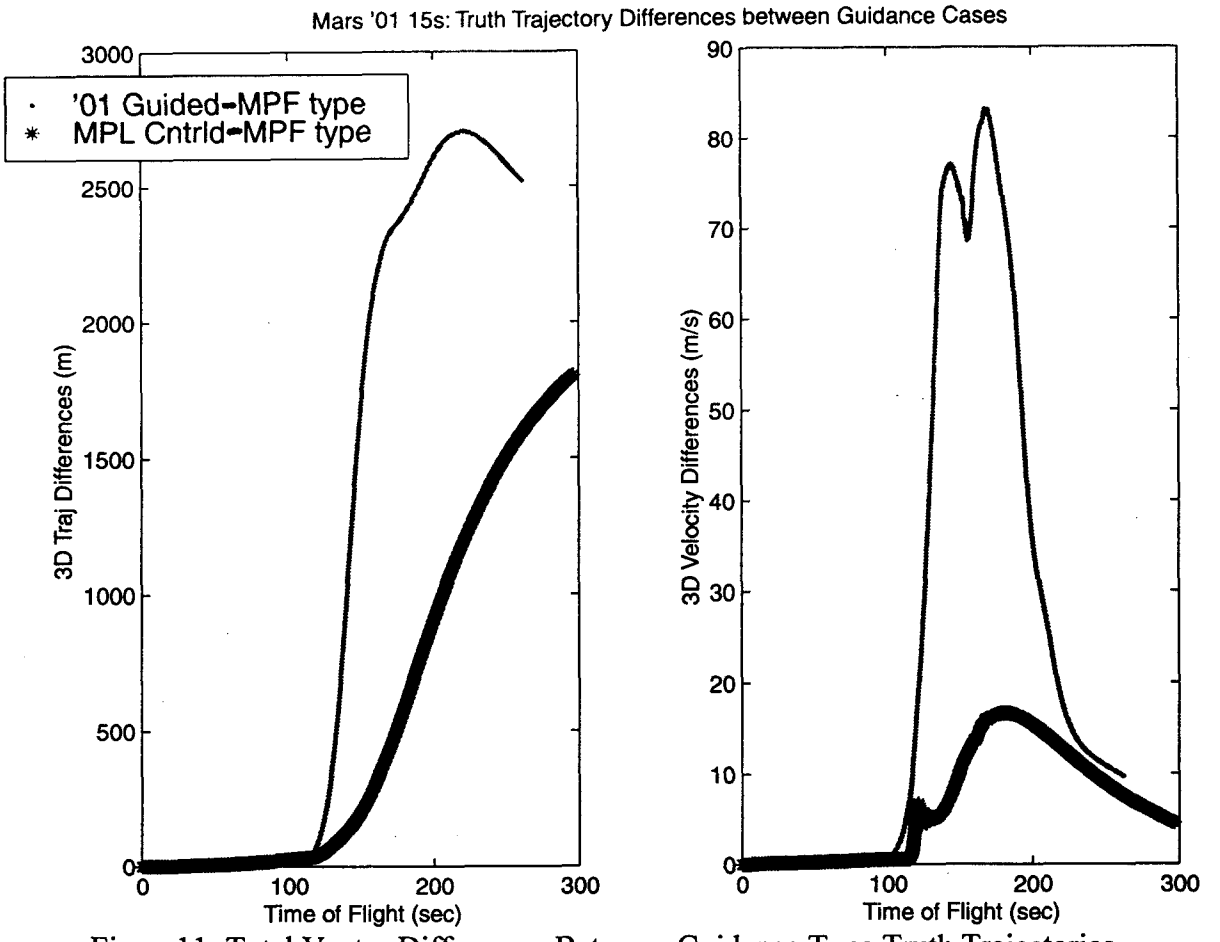

Figure11: Total Vector Differences Between Guidance Type Truth Trajectories

SUMMARY OF RESULTS

Reconstructed trajectories for all entry cases analyzed (guided, un-guided but controlled, and ballistic) display the same signatures in the differences with respect to the "True" trajectory. During the hypersonic phase of entry as the drag forces rapidly increase in magnitude the reconstructed position difference increases with a near linear trend. Correspondingly, velocity differences progress though a chaotic transient interval until they effectively settle into velocity 'biases'. In general, this signature can be attributed to accumulation of non-linear errors arising from propagation along an incorrect trajectory whose 'dynamics' are dominated by non-conservative forces, such as, atmospheric drag.

A 'trade-off' between frequencies of available "Quick-Look" NAV data and the accuracies of their corresponding reconstructed trajectories exists. As expected, decreasing the NAV data rates reduces estimated trajectory accuracies. Apparently, this degradation is due to the loss of high frequency information in the accelerometer time series. An array of attempts at varying the processing of the Quick-Look NAV data could not mitigate this loss of accuracy from less frequent NAV data. Techniques analyzed included smoothing out high

frequency signal in the QL NAV data, reinterpolation to higher frequencies, and changing integrator characteristics.

A reasonable break point in reconstruction accuracies would be Quick Look NAV data at 1.5s spacing; with more complex guidance schemes benefiting the most from higher frequency NAV data. However, further analysis on the effect of data drop-outs is necessary before final determination for sophisticated guidance scenarios. Results for the MPL type data at the 1.5 s interval suggests that the greatest benefit from Quick Look NAV data occurs at intervals near the aerobody's natural oscillation frequency.

It must be noted that the total error in a entry probe's estimated trajectory, is obtained by adding the above mentioned Quick Look NAV data reconstruction uncertainties to the pre-existing current mission state uncertainty.

The presence of AES simulated data's synthetic sensor noise effectively smooths, through 'whitening', the sample Quick Look NAV data. These DR reconstructions are very similar to and sometimes even out perform reconstructions using perfect data. Thus, to the extent that they are appropriately characterized, NAV sensor measurement errors are not a limiting characteristic in "Quick-Look" entry reconstruction trajectories.

Much of the larger differences observed in the "Guided" type entry's decent and downrange components, in comparison with the MPL and MPF entry types, is apparently NOT due to the higher frequency structure in the acceleration time series (arising from more dynamic attitude changes). Rather the differences are from the presence of larger lift forces' variability which present greater opportunity for the DR integrator to progress along the wrong trajectory, thus giving rise to greater non-linear errors. However, even at the most rarefied 2sec QL NAV data sampling interval the errors in the reconstructed trajectories are smaller than the trajectory differences occurring from different entry guidance scenarios. Thus, more intricate entry guidance scenarios are not a limiting factor in the "Quick-Look" entry reconstruction trajectories.

FURTHER STUDY

Several areas of further study have been identified. These areas include the following:

• Analyze reconstructed trajectory sensitivity to temporal data dropouts of all or part of the navigation data set or premature data termination. Include the effect where error rates are correlated with 'truth' navigation and attitude dynamics (e.g., data dropout rates are increased with acceleration magnitudes) or there exists observation thresholds (e.g., no data above specified spin rates).

• Verify current observation of low susceptibility to the presence of NAV measurement noise by further tests with additional AES simulation dispersion cases.

• Characterize solution stability, and possible anomaly detection capability, by running large dispersion 'robustness' cases which include the effects of various combinations of anomalously large dynamic and measurement errors present in: atmospheric forces, sensor

errors (including failure modes), guidance/control, aerodynamics, and entry navigation uncertainty conditions.

• Test current NAV measurement noise model characterizations by analyzing high-frequency signal and noise available in MPF entry accelerometer data.

• Quantify the benefit from incorporating measurements from other sensors including: DSN direct tracking radiometric data, and "in situ" data such as radar velocity or attitude measurements taken from sensors on-board the Mars entry lander.

• Identify and track observational channels response to errors. Solution recovery levels of confidence can be based on the channels' sensitivities and performance to known error sources. State solution and channel performances to anticipated errors and to the presence of especially large dispersions (referred to as robustness cases) are discussed. For example, the ability to 'back-out' atmospheric and aerodynamic effects, while varying the dynamic and measurement errors, is presented.

• Investigate sensitivity in "Quick-Look" NAV reconstruction accuracies to aerodynamic and/or atmospheric miss-modeling or mischaracterization.

ACKNOWLEDGEMENTS

This research was supported by NASA contract NAS9-97045.

REFERENCES

1. Striepe, S., et. al.; "An Atmospheric Guidance Algorithm Testbed for the Mars Surveyor Program 2001 Orbiter and Lander," AIAA 98-4569, Aug. 1998.

2. Spencer, D.A., R.C. Blanchard, R.D. Braun, P.H. Kallemeyn, and S.W. Thurman, "Mars Pathfinder Entry, Descent, and Landing Reconstruction," *Journal of Spacecraft and Rockets*, Vol.36, No. 3, 1999, pp. 357-3

3. Shampine, L. and M. Gordon, Computer Solution of Ordinary Differential Equations, The Initial Value Problem, W. H. Freeman and Company, San Francisco, 1975.

4. Vondrak, J., "A Contribution to the Problem of Smoothing Observational Data," *Bull. Astron. Inst. Czech.*, Vol 20, Pg 349, 1969.